Mon. Not. R. astr. Soc. (1967) **137**, 311–335.

THE TROJAN MANIFOLD IN THE SYSTEM EARTH–MOON

André Deprit, Jacques Henrard, Julian Palmore and J. F. Price

(Communicated by D. H. Sadler)

(Received 1967 April 3)

Summary

The Trojan manifold is defined as the analytical manifold of periodic orbits which contains the triangular equilibrium L_4 as a singularity.

Two branches emanate from L_4: the branch $\mathscr{L}_4{}^l$ of long period orbits and the branch $\mathscr{L}_4{}^s$ of short period orbits. $\mathscr{L}_4{}^l$ terminates on a bifurcation orbit which is a short period orbit; $\mathscr{L}_4{}^s$ terminates on a symmetrical periodic orbit which belongs both to the branch $\mathscr{L}_5{}^s$ of short period orbits emanating from the equilibrium L_5 and to the branch $\mathscr{L}_3$ of periodic librations around the collinear equilibrium L_3.

1. *Introduction.* Let us identify the system Earth–Moon with a planar restricted problem of three bodies. The barycentric synodical coordinate system and the units of length, time and mass are chosen as defined by Wintner (1941); the mass ratio μ is taken equal to 0·012150. For this value, the triangular configuration of equilibrium, usually denoted by L_4, is stable, and it generates two natural families of periodic orbits.

The continuation of these families to their natural terminations is no longer an exercise of academic interest. Recently the stability of the Lagrangian equilibrium point L_4 in the system Earth–Moon has received a great deal of attention (Breakwell & Pringle 1966, Steg & de Vries 1966, Schutz 1966). A theory of the motions around L_4 starts much in the same way as that of the Trojan orbits: discarding all other forces as perturbations, one aims at constructing as an intermediate orbit an asymptotic representation of the motion about L_4 in the simplified model which is the Restricted Problem. Such approximations are hard to come by, and, because of the many restrictive assumptions on which they are built, they ought to be checked carefully and their domains of validity should be circumscribed accurately. One way of testing such theories is to investigate how faithfully they reproduce the two natural families of periodic orbits emanating from the triangular equilibrium itself.

In this respect, the difficulty is that the present literature in celestial mechanics does not provide enough information on the genealogy of these families. A few elements of the family $\mathscr{L}_4{}^l$ of long period orbits in the immediate neighbourhood of the point L_4 have been computed by Rabe & Schanzle (1962); their investigations have been extended a few steps further by Wolaver (1963). As for the branch $\mathscr{L}_4{}^s$ of short period orbits, nothing definite is known about it beyond the analytical continuation carried out by Pedersen (1935) up to order 3 and Birkhoff's normalization performed up to order 12 (Deprit, Henrard & Rom 1967).

This paper presents the *complete* history of both branches $\mathscr{L}_4{}^l$ and $\mathscr{L}_4{}^s$. In point of fact, we begin by expanding the two families in d'Alembert series of a regularizing orbital parameter ϵ. The development shows that, on each branch, the equilibrium itself stands as a ramification point whose index is equal to 2;

From those properties we conclude that

$$X(\tau, -\epsilon)=X(\tau+\pi, \epsilon)$$

$$Y(\tau, -\epsilon)=Y(\tau+\pi, \epsilon).$$

As a result the value of the Hamiltonian function (2) is a power series in the square of the orbital parameter

$$h=\sum_{m\geqslant 1} h_{2m}\epsilon^{2m}. \tag{7}$$

From these remarks it is not difficult to show that:

(a) The families issuing from L_4 are natural families of periodic orbits, except at the equilibrium point L_4 which is a singularity;

(b) The orbital parameter is an analytical coordinate which renders uniform the local equilibrium;

(c) Each of the families admits a unique real continuation through the equilibrium ($\epsilon=0$), but it is a reflection of the branch upon itself.

The expansions (3) and (5) can be performed automatically on a computer up to a high order. When the program is based on the method of undetermined coefficients, one can for instance take advantage of the fact that the series $X(\tau, \epsilon)$ and $Y(\tau, \epsilon)$ have the d'Alembert characteristic. It is then possible to write down explicitly the recurrent systems of linear equations to be satisfied at each order by the various coefficients in the series. At each order, the right-hand members of the systems and their solutions are constructed by manipulating subscripted variables (Deprit & Delie 1965). But we can also proceed in a more global way. The basic constituents of the program are no longer the coefficients of the trigonometric lines in the terms $X_m(\tau)$ and $Y_m(\tau)$, but simply these trigonometric sums themselves. They are manipulated as elements of an algebra. The program calls subroutines which assemble these basic cells according to the usual laws of composition in the algebra of Fourier sums (Danby *et al.* 1965).

We shall outline here the main steps of this computation. The Lagrangian differential equations associated with the Hamiltonian (2) are:

$$\begin{aligned}(\omega_0{}^2D^2-\tfrac{3}{4})X-D_1Y&=F(\nu; X, Y),\\ (\omega_0{}^2D^2-\tfrac{9}{4})Y+D_2X&=G(\nu; X, Y),\end{aligned} \tag{8}$$

where

$$D_1=2\omega_0 D+\frac{3\sqrt{3}}{2}\left(\tfrac{1}{2}-\mu\right),$$

$$D_2=2\omega_0 D-\frac{3\sqrt{3}}{2}\left(\tfrac{1}{2}-\mu\right).$$

The operator D is the operator of differentiation with respect to the time τ; the right-hand members are

$$F(\nu; X, Y)=\nu D_1Y+\frac{3}{2}\nu X+\nu^2\left[\frac{3}{4}X+\frac{3\sqrt{3}}{2}\left(\frac{1}{2}-\mu\right)Y\right]+(1+\nu)^2\left(\frac{\partial}{\partial X}\sum_{p\geqslant 3}\Omega_p\right),$$

$$G(\nu; X, Y)=-\nu D_2X+\frac{9}{2}\nu Y+\nu^2\left[\frac{3}{4}Y+\frac{3\sqrt{3}}{2}\left(\frac{1}{2}-\mu\right)X\right]+(1+\nu)^2\left(\frac{\partial}{\partial Y}\sum_{p\geqslant 3}\Omega_p\right).$$

Introducing the formal expansions (3) and (5) into equations (8) enables us to solve the system by recurrence. Let us observe that, once we know the expansions

Problem of Three Bodies is described by the Hamiltonian function

$$H=\frac{1}{2}(P_x^2+P_y^2)-(xP_y-yP_x)-\frac{1-\mu}{\rho_1}-\frac{\mu}{\rho_2}, \tag{1}$$

where

$$\rho_1^2=(x+\mu)^2+y^2,$$
$$\rho_2^2=(x+\mu-1)^2+y^2.$$

The transformation

$$x=\tfrac{1}{2}-\mu+X, \qquad P_x=-\tfrac{1}{2}\sqrt{3}+P_X,$$
$$y=\tfrac{1}{2}\sqrt{3}+Y, \qquad P_y=\tfrac{1}{2}-\mu+P_Y,$$

is a conservative completely canonical mapping of the phase space (x, y, P_x, P_y) onto the phase space (X, Y, P_X, P_Y), the origin of which is the equilibrium point L_4. The Hamiltonian function (1) becomes

$$H=\tfrac{1}{2}(P_X^2+P_Y^2)-(XP_Y-YP_X)-\Omega \tag{2}$$

where the force function $\Omega(X, Y)$ is defined by

$$\Omega=\left(\frac{1}{2}-\mu\right)X+\frac{\sqrt{3}}{2}Y+\frac{1-\mu}{\rho_1}+\frac{\mu}{\rho_2}-1.$$

We expand Ω in power series of X, Y,

$$\Omega=\sum_{p\geq 2}\Omega_p(X, Y),$$

Ω_p denoting the homogeneous polynomial component of order p in X, Y.

It is known that, for the system Earth–Moon where $\mu=0\cdot012150$, two families of periodic orbits issue from L_4. In the neighbourhood of L_4, each family can be expanded in power series of an orbital parameter ϵ

$$\begin{aligned} X(\tau, \epsilon)&=\sum_{m\geq 1}X_m(\tau)\epsilon^m \\ Y(\tau, \epsilon)&=\sum_{m\geq 1}Y_m(\tau)\epsilon^m. \end{aligned} \tag{3}$$

The function $X_m(\tau)$ and $Y_m(\tau)$ are Fourier sums in τ which is a new time variable defined by the relation

$$\tau=\frac{\omega_0}{1+\nu}t, \tag{4}$$

where $i\omega_0$ is one of the characteristic exponents at the equilibrium (the other one being $i\lambda_0$) and the correction ν to the period is a power series in the orbital parameter

$$\nu=\sum_{m\geq 1}\nu_m\epsilon^m. \tag{5}$$

The coefficients in the power series (3) and (5) have the following parity properties (Deprit & Delie 1965):

$$X_{2p}(\tau+\pi)=X_{2p}(\tau), \qquad Y_{2p}(\tau+\pi)=Y_{2p}(\tau), \tag{6a}$$
$$X_{2p+1}(\tau+\pi)=-X_{2p+1}(\tau), \qquad Y_{2p+1}(\tau+\pi)=-Y_{2p+1}(\tau), \tag{6b}$$
$$\nu_{2p+1}=0. \tag{6c}$$

but it turns out that the real continuation of the branch through the singularity is a reflection of the class upon itself. Consequently, for both families, the equilibrium point L_4 is a *natural termination.*

For $\mathscr{L}_4{}^l$, we have found that a maximum value is reached for the Jacobi constant C. At this point, the characteristic exponents become of the unstable type and will remain so until the end of the family. While the Jacobian constant decreases strictly monotonically, the orbits develop three inner loops. Eventually the three loops come to coincidence: the last long period orbit ' shrinks ' to a short period orbit travelled four times. Let us call this bifurcation orbit B_1.

The standard conjectures concerning the genealogy of $\mathscr{L}_4{}^l$ were such as to rule out the existence of B_1. Brown's fundamental paper (Brown 1911, Brown & Shook 1933) indicates considerations to the effect that, if the Jacobi constant C approaches its value at the collinear equilibrium L_3, then $\mathscr{L}_4{}^l$ must tend to an orbit doubly asymptotic to this equilibrium, usually referred to as the *limiting orbit.* It was suggested that $\mathscr{L}_4{}^l$ could be continued beyond the limiting orbit by a branch of symmetrical periodic orbits in the shape of horseshoes. That such a horseshoe-shaped orbit has been obtained by Rabe as a result of his continuation procedure along $\mathscr{L}_4{}^l$ is held by Stumpff (1965) as a very strong indication that the family $\mathscr{L}_4{}^l$ evolves according to Brown's conjecture.

We contend here that this interpretation fails at least in the system Earth–Moon and also, as we show it elsewhere, for Routh's critical mass ratio. The evidence we bring is purely numerical; thus from the rigorous mathematical point of view, the global genealogy of the long period branch $\mathscr{L}_4{}^l$ remains an unsolved problem and we do not suggest that it is likely to be an easy one. Nevertheless, our numerical methods are justified rigorously and the results they produced have been checked throughout.

The existence of the bifurcation orbit B_1 invites us to revise our terminology. Strictly speaking, $\mathscr{L}_4{}^l$ and $\mathscr{L}_4{}^s$ should no longer be considered as two distinct analytical families of periodic orbits, but rather as two distinct branches of a unique analytical manifold. As it can be characterized as the hypersurface containing the equilibrium L_4 as an essential singularity, it will be called the Trojan manifold (even when μ is not the mass ratio of the system Sun–Jupiter).

The branch $\mathscr{L}_4{}^s$ has a simple history, but a surprising end. Along it the Jacobi constant decreases monotonically and the characteristic exponents maintain their stable character throughout. Eventually $\mathscr{L}_4{}^s$ reaches an orbit (B_2) which is symmetric with respect to the axes of syzygies. At B_2, $\mathscr{L}_4{}^s$ meets the branch $\mathscr{L}_5{}^s$ of short period orbits emanating from the equilibrium L_5; we further show that B_2 belongs also to the branch $\mathscr{L}_3$ of periodic orbits emanating from the equilibrium point L_3.

At a time when the termination for a natural family of periodic orbits had not yet been given a sharp mathematical definition, Brown suggested that the branch $\mathscr{L}_4{}^s$ would end with a collision orbit (E_1) out of the more massive primary. We confirm here that such an orbit exists on the Trojan manifold, but it is reached only after the branches $\mathscr{L}_4{}^s$, $\mathscr{L}_5{}^s$ have met on an element of $\mathscr{L}_3$; besides E_1 corresponds to the collision orbit computed by Burrau (1894) when the mass ratio is equal to 1/2.

2. *Analytical expansion around* L_4. In the barycentric synodical coordinate system, with the usual canonical units (Wintner 1941), the planar Restricted

(3) and (5) up to order N in ϵ, we are able to compute the Fourier sums $F_N(\tau)$, $G_N(\tau)$ which are the coefficients of ϵ^N in the expansion of the right-hand members of (8). In order to find X_N and Y_N we then have to solve the differential system:

$$\begin{aligned}(\omega_0{}^2D^2-\tfrac{3}{4})X_N-D_1Y_N&=F_N(\tau),\\(\omega_0{}^2D^2-\tfrac{9}{4})Y_N+D_2X_N&=G_N(\tau).\end{aligned}\tag{9}$$

By differentiating and combining the equations (9), we obtain the differential relations

$$\begin{aligned}\omega_0{}^2(D^2+1)(\omega_0{}^2D^2+\lambda_0{}^2)X_N&=\phi_N(\tau),\\\omega_0{}^2(D^2+1)(\omega_0{}^2D^2+\lambda_0{}^2)Y_N&=\psi_N(\tau),\end{aligned}\tag{10}$$

to be satisfied by any solution of (9). In equation (10), we have put

$$\begin{aligned}\phi_N(\tau)&=(\omega_0{}^2D^2-\tfrac{9}{4})F_N(\tau)+D_1G_N(\tau),\\\psi_N(\tau)&=(\omega_0{}^2D^2-\tfrac{3}{4})G_N(\tau)-D_2F_N(\tau).\end{aligned}\tag{11}$$

Let us assume that $F_N(\tau)$ and $G_N(\tau)$ do not contain terms in $\cos\tau$ or $\sin\tau$. The formal integration of (10)

$$\begin{aligned}X_N{}^*&=\frac{1}{\omega_0{}^2(D^2+1)(\omega_0{}^2D^2+\lambda_0{}^2)}\,\phi_N(\tau),\\Y_N{}^*&=\frac{1}{\omega_0{}^2(D^2+1)(\omega_0{}^2D^2+\lambda_0{}^2)}\,\psi_N(\tau),\end{aligned}\tag{12}$$

yields a particular solution of equation (9). By definition, the inverse differential operator in equation (12) transforms terms like $A\cos n\tau$ and $B\sin n\tau$ into the terms

$$\frac{A}{\omega_0{}^2(n^2-1)(\omega_0{}^2n^2-\lambda_0{}^2)}\cos n\tau,\qquad\frac{B}{\omega_0{}^2(n^2-1)(\omega_0{}^2n^2-\lambda_0{}^2)}\sin n\tau,$$

respectively (provided of course that $n\neq 1$).

In order to discuss the solution of the differential system (9) we have to consider two cases.

A: the order N reached by the recurrence is even: $N=2M$

The recurrence implies that $F_{2M}(\tau)$ and $G_{2M}(\tau)$ are known Fourier sums and, in view of the parity conditions (6), they have the parity properties

$$F_{2M}(\tau+\pi)=F_{2M}(\tau),\qquad G_{2M}(\tau+\pi)=G_{2M}(\tau).$$

Hence the particular solution $X_{2M}{}^*(\tau)$, $Y_{2M}{}^*(\tau)$ obtained from (12) possesses the parity property (6a). As a matter of fact it is the only solution of (9) having this characteristic. Thus at an even order, it is sufficient to take

$$X_{2M}(\tau)=X_{2M}{}^*(\tau),\qquad Y_{2M}(\tau)=Y_{2M}{}^*(\tau).$$

B: $N=2M+1$ is odd

As we did not determine the coefficient ν_{2M} at the preceding step, the recurrence implies that

$$\begin{aligned}F_{2M+1}(\tau)&=F_{2M+1}{}^*(\tau)+\tilde{F}_{2M+1}(\nu_{2M},\tau)\\G_{2M+1}(\tau)&=G_{2M+1}{}^*(\tau)+\tilde{G}_{2M+1}(\nu_{2M},\tau)\end{aligned}\tag{13}$$

where $\tilde{F}_{2M+1}$ and $\tilde{G}_{2M+1}$ contain only terms in cos τ and sin τ whose coefficients depend linearly on ν_{2M} whereas $F_{2M+1}{}^*$ and $G_{2M+1}{}^*$ are Fourier sums, lacking terms in cos τ and sin τ and with the property that

$$F_{2M+1}{}^*(\tau) = -F_{2M+1}{}^*(\tau+\pi), \qquad G_{2M+1}{}^*(\tau) = -G_{2M+1}{}^*(\tau+\pi).$$

Hence a particular solution of the differential system (9) is to be decomposed into the sums

$$\begin{aligned} X_{2M+1}(\tau) &= X_{2M+1}{}^*(\tau) + \tilde{X}_{2M+1}(\tau), \\ Y_{2M+1}(\tau) &= Y_{2M+1}{}^*(\tau) + \tilde{Y}_{2M+1}(\tau). \end{aligned} \tag{14}$$

The functions $X_{2M+1}{}^*(\tau)$, $Y_{2M+1}{}^*(\tau)$ are particular solutions of the system (9) in which the right-hand members are $F_{2M+1}{}^*(\tau)$, $G_{2M+1}{}^*(\tau)$:

$$\begin{aligned} (\omega_0{}^2D^2 - \tfrac{3}{4})X_{2M+1}{}^* - D_1 Y_{2M+1}{}^* &= F_{2M+1}{}^*(\tau), \\ (\omega_0{}^2D^2 - \tfrac{9}{4})Y_{2M+1}{}^* + D_2 X_{2M+1}{}^* &= G_{2M+1}{}^*(\tau), \end{aligned} \tag{15}$$

while $\tilde{X}_{2M+1}(\tau)$, $\tilde{Y}_{2M+1}(\tau)$ are particular solutions of

$$\begin{aligned} (\omega_0{}^2D^2 - \tfrac{3}{4})\tilde{X}_{2M+1} - D_1\tilde{Y}_{2M+1} &= \tilde{F}_{2M+1}(\tau), \\ (\omega_0{}^2D^2 - \tfrac{9}{4})\tilde{Y}_{2M+1} + D_2\tilde{X}_{2M+1} &= \tilde{G}_{2M+1}(\tau). \end{aligned} \tag{16}$$

On the one hand, a particular solution $X_{2M+1}{}^*(\tau)$, $Y_{2M+1}{}^*(\tau)$ of (15), possessing the parity property (6b) is readily found by the formal integration (12). On the other hand, the system (16) has periodic solutions if and only if the combinations $\tilde{\phi}_{2M+1}(\tau)$ and $\tilde{\psi}_{2M+1}(\tau)$, defined as in (11) by means of $\tilde{F}_{2M+1}(\tau)$ and $\tilde{G}_{2M+1}(\tau)$, lack terms in cos τ and sin τ. The elimination of these critical terms leads to two linear equations in the coefficient ν_{2M} of the period. In theory, Lyapunov's theorem proves that this system is consistent, resulting in one and only one value for ν_{2M} (Nemytskii & Stepanov, p. 216). In practice, we solve each equation separately for ν_{2M}, the disagreement between the two roots being an indication of the absolute accuracy which remains in the computation at order $N = 2M+1$.

This being done, it remains to find a particular solution of the system (16); we found it convenient to postulate that it be of the form

$$\tilde{X}_{2M+1}(\tau) = A \sin \tau, \qquad \tilde{Y}_{2M+1}(\tau) = B \cos \tau. \tag{17}$$

The coefficients A and B are readily computed by substituting equation (17) into equation (16).

We have just outlined a recurrence scheme by which one can implement on a computer the expansion of the short and long period families in the neighbourhood of the equilibrium L_4. The expansion has been carried up to order 14 in ϵ for the short period orbits and, because the numerical convergence is less favourable in this case, up to order 29 in ϵ for the long period orbits. We give in Tables I and II the expansions of the Jacobian constant C, and the mean motion ω

$$C = 3 - \frac{h}{2}, \qquad \omega = \frac{\omega_0}{1+\nu}. \tag{18}$$

A third column contains the test we have mentioned above on the absolute accuracy of the coefficients of ω. Note that, as far as we have determined them, the series for the long period orbits appear to be alternate and are of poor numerical convergence. The truncation errors are then difficult to appreciate for values of ϵ

TABLE I

Series for the short period orbits

	Jacobi constant	Mean motion ω	Test on ω
ϵ^0	3	0·95450323	—
ϵ^2	$-1\cdot90900646\times10^{-2}$	$2\cdot31356090\times10^{-3}$	4×10^{-17}
ϵ^4	$2\cdot30820785\times10^{-5}$	$-9\cdot40258657\times10^{-5}$	2×10^{-17}
ϵ^6	$1\cdot65647506\times10^{-4}$	$-1\cdot44527659\times10^{-5}$	8×10^{-18}
ϵ^8	$-2\cdot04333857\times10^{-5}$	$3\cdot61295288\times10^{-6}$	1×10^{-18}
ϵ^{10}	$-2\cdot33405689\times10^{-6}$	$-1\cdot29048091\times10^{-8}$	3×10^{-19}
ϵ^{12}	$1\cdot03763323\times10^{-6}$	$-1\cdot26602509\times10^{-7}$	1×10^{-20}
ϵ^{14}	$-5\cdot23923254\times10^{-8}$	—	—

TABLE II

Series for the long period orbits

	Jacobi constant	Mean motion ω	Test on ω
ϵ^0	3	0·29820058	—
ϵ^2	$4\cdot80738160\times10^{-3}$	$-5\cdot45844525\times10^{-3}$	2×10^{-15}
ϵ^4	$7\cdot39602152\times10^{-4}$	$9\cdot04904192\times10^{-3}$	4×10^{-16}
ϵ^6	$-1\cdot01881203\times10^{-3}$	$-2\cdot92749334\times10^{-3}$	3×10^{-16}
ϵ^8	$1\cdot84262434\times10^{-5}$	$6\cdot27080608\times10^{-4}$	2×10^{-16}
ϵ^{10}	$-6\cdot86021705\times10^{-4}$	$-2\cdot77040703\times10^{-3}$	2×10^{-16}
ϵ^{12}	$4\cdot39315127\times10^{-4}$	$1\cdot19612069\times10^{-3}$	2×10^{-16}
ϵ^{14}	$-4\cdot26041142\times10^{-4}$	$-2\cdot90917642\times10^{-3}$	2×10^{-16}
ϵ^{16}	$7\cdot34830864\times10^{-4}$	$1\cdot35200937\times10^{-3}$	5×10^{-17}
ϵ^{18}	$-4\cdot95099685\times10^{-4}$	$-3\cdot17046609\times10^{-3}$	5×10^{-16}
ϵ^{20}	$9\cdot74187343\times10^{-4}$	$2\cdot27427517\times10^{-3}$	8×10^{-17}
ϵ^{22}	$-7\cdot59026422\times10^{-4}$	$-3\cdot72703143\times10^{-3}$	5×10^{-18}
ϵ^{24}	$1\cdot26481911\times10^{-3}$	$3\cdot58905462\times10^{-3}$	8×10^{-17}
ϵ^{26}	$-1\cdot24422884\times10^{-3}$	$-4\cdot76832208\times10^{-3}$	5×10^{-16}
ϵ^{28}	$1\cdot71821060\times10^{-3}$	$5\cdot57227739\times10^{-3}$	4×10^{-16}

large enough to produce non-negligible contributions in the last orders and one has to be careful in using the truncated series. To illustrate this difficulty, we compare in Fig. 1 the period curve of the long period orbits with its estimates from either Birkhoff's normalization truncated at order 12 (Deprit *et al.* 1967)

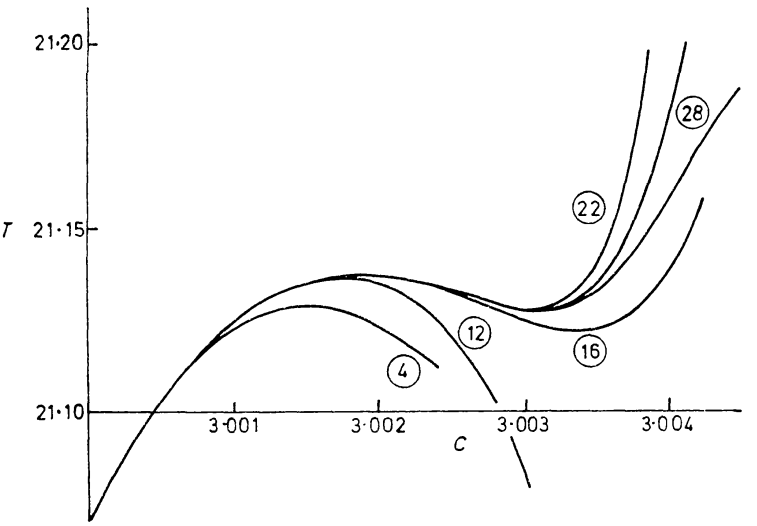

FIG. 1. *The period curve for $\mathcal{L}_4^1$ and its asymptotic estimates to various orders.*

or the series in Table II truncated at increasing orders. The greater the order, the larger the interval of C on which the period curve coincides with its estimate. It is quite striking to see that unless it is expanded beyond order 15 in ϵ, the series (5) does not reveal that the period goes through two relative extrema.

3. *Numerical continuation in cartesian coordinates.* The analytical expansion around L_4 enables us to compute the long period orbits up to a value of the Jacobi constant $C=3\cdot003$ and the short period orbits down to about $C=2\cdot95$. Thus, beyond those values, the two natural families should be continued numerically. For that purpose, we use a predictor–corrector scheme (Deprit–Henrard 1967) based upon the numerical integration of Hill's equation. Suppose we know a trajectory $x(t)$, $y(t)$ of the restricted problem, i.e. a solution of the Lagrangian equations

$$\begin{aligned} \ddot{x}-2\dot{y}&=W_x,\\ \ddot{y}+2\dot{x}&=W_y, \end{aligned} \tag{19}$$

where

$$W=\frac{1}{2}(x^2+y^2)+\frac{1-\mu}{\rho_1}+\frac{\mu}{\rho_2}. \tag{20}$$

The trajectory belongs to the manifold

$$C_0=2W(x,y)-(\dot{x}^2+\dot{y}^2) \tag{21}$$

where the numerical quantity C_0 is the value of the Jacobi constant.

A nearby trajectory

$$X=x(t)+u(t), \qquad Y=y(t)+v(t), \tag{22}$$

for which the Jacobi constant has the value C, will be described by its normal and tangential displacements

$$\begin{aligned} n(t)&=-u(t)\sin\phi(t)+v(t)\cos\phi(t),\\ p(t)&=u(t)\cos\phi(t)+v(t)\sin\phi(t), \end{aligned} \tag{23}$$

with respect to the known trajectory; the angle ϕ is a function of the time defined by the relations

$$\begin{aligned} \dot{x}(t)&=V(t)\cos\phi(t),\\ \dot{y}(t)&=V(t)\sin\phi(t), \end{aligned} \tag{24}$$

provided the velocity $V(t)$ does not vanish at any time along the orbit. Let us make the assumption that the squares of the displacements are negligible. Hence the normal displacement is a solution of the non-homogeneous Hill's equation

$$\ddot{n}+\theta n=2\gamma(1+\dot{\phi})/V. \tag{25}$$

The coefficient θ is a function of the time defined by

$$\theta=\ddot{V}/V+2(1+\dot{\phi})^2-(1-\mu)/\rho_1{}^3-\mu/\rho_2{}^3, \tag{26}$$

and is thus to be computed along the trajectory $x(t)$, $y(t)$. The numerical quantity γ measures the variation of the Jacobi constant

$$\gamma=\tfrac{1}{2}(C-C_0)=p\ddot{V}-\dot{p}V+2V(1+\dot{\phi})n, \tag{27}$$

due to the displacement from the basic orbit.

The general solution of the non-homogeneous Hill's equation (25) is

$$n(t)=\alpha n_1(t)+\beta n_2(t)+\gamma n_3(t), \tag{28}$$

where $n_1(t)$ and $n_2(t)$ are the particular solutions of Hill's equation

$$\ddot{n}+\theta n=0 \tag{29}$$

meeting the initial conditions

$$n_1(0)=1, \qquad \dot{n}_1(0)=0,$$
$$n_2(0)=0, \qquad \dot{n}_2(0)=1.$$

The function $n_3(t)$ is the particular solution of

$$\ddot{n}+\theta n=2(1+\dot{\phi})/V, \tag{30}$$

defined by the initial conditions

$$n_3(0)=0, \qquad \dot{n}_3(0)=0.$$

To each normal displacement $n(t)$ corresponds a tangential displacement $p(t)$ (with $p(0)=0$) given by the quadrature

$$p(t)=V(t)\int_0^t\left[2\,\frac{1+\dot{\phi}(s)}{V(s)}\,n(s)-\frac{\gamma}{V^2(s)}\right]ds; \tag{31}$$

hence it consists of the linear combination

$$p(t)=\alpha p_1(t)+\beta p_2(t)+\gamma p_3(t). \tag{32}$$

Let us assume that the basic trajectory $x(t)$, $y(t)$ is close to being periodic; i.e. the quantities

$$\begin{aligned}\Delta x&=x(T)-x(0), \qquad \Delta\dot{x}=\dot{x}(T)-\dot{x}(0)\\ \Delta y&=y(T)-y(0), \qquad \Delta\dot{y}=\dot{y}(T)-\dot{y}(0)\end{aligned} \tag{33}$$

are small for some given value, say $T>0$, of the time. For a displacement (22) of the orbit to be periodic with period $T+\Delta T$, it is necessary that α, β and ΔT be solutions of the linear system

$$\begin{aligned}\alpha[n_1(T)-1]+\beta n_2(T)+\gamma n_3(T)&=\Delta_1\\ \alpha\dot{n}_1(T)+\beta[\dot{n}_2(T)-1]+\gamma\dot{n}_3(T)&=\Delta_2\\ \alpha p_1(T)+\beta p_2(T)+\gamma p_3(T)+V_0\Delta T&=\Delta_3,\end{aligned} \tag{34}$$

where

$$\Delta_1=\Delta x\sin\phi(0)-\Delta y\cos\phi(0),$$
$$\Delta_2=[\Delta\dot{x}+\dot{\phi}(0)\Delta y]\sin\phi(0)-[\Delta\dot{y}-\dot{\phi}(0)\Delta x]\cos\phi(0),$$
$$\Delta_3=-\Delta x\cos\phi(0)-\Delta y\sin\phi(0).$$

Predictor. Let us start from a periodic orbit of period T. The problem is to find an estimate of the initial conditions for the periodic orbits which continue this given orbit in the neighbourhood of C_0. This problem reduces to solving in terms of γ the system (34) in which the right-hand members are precisely zero by virtue of our assumptions. Let this solution be

$$\alpha=\alpha^*\gamma, \qquad \beta=\beta^*\gamma, \qquad \Delta T=\Delta T^*\gamma.$$

Thus in order to get an estimate of the initial conditions and of the period of the nearby periodic orbit with $C=C_0+2\gamma$, we augment the initial conditions and the period by the quantities

$$\Delta x_0=2\frac{\partial x_0}{\partial C}\gamma=-2\gamma\alpha^*\sin\phi(0),$$

$$\Delta y_0=2\frac{\partial y_0}{\partial C}\gamma=2\gamma\alpha^*\cos\phi(0),$$

$$\Delta\dot{x}_0=2\frac{\partial\dot{x}_0}{\partial C}\gamma=2\gamma\{-\beta^*\sin\phi(0)+[\alpha^*(\dot{\phi}(0)+2)+1/V(0)]\cos\phi(0)\},\tag{35}$$

$$\Delta\dot{y}_0=2\frac{\partial\dot{y}_0}{\partial C}\gamma=2\gamma\{\beta^*\cos\phi(0)+[\alpha^*(\dot{\phi}(0)+2)+1/V(0)]\sin\phi(0)\},$$

$$\Delta T=2\frac{dT}{dC}\gamma=-\frac{2\gamma}{V(0)}\{\alpha^*p_1(T)+\beta^*p_2(T)+p_3(T)\}.$$

The notation of partial differentiation comes from the fact that in the vicinity of the initial point of the periodic orbits $x(t)$, $y(t)$ the manifold of periodic orbits can be mapped in theory by two analytical coordinates, one being the time along the orbit (provided of course that an initial point has been suitably chosen on each periodic orbit), the other one (across the orbits) being the Jacobi constant C.

This first order predictor breaks down when the determinant

$$\begin{vmatrix} n_1(T)-1 & n_2(T) & 0 \\ \dot{n}_1(T) & \dot{n}_2(T)-1 & 0 \\ p_1(T) & p_2(T) & V(0) \end{vmatrix}=V(0)[n_1(T)+\dot{n}_2(T)-2]\tag{36}$$

of system (34) is zero. To cast some light on these critical cases, we examine all the other determinants of order 3 which we can extract from the left-hand member of system (34). None of them is zero unless

$$\dot{n}_3(T)[n_1(T)-1]-n_3(T)\dot{n}_1(T)\tag{37}$$

is zero, in which case all of them would also be zero. In the case when equation (37) is not zero, the Jacobi constant C considered as a function of the orbital parameter defining the family becomes stationary along the basic orbit; but the family can be continued numerically, in one way only, beyond this non-essential singularity. By contrast, when the determinant (37) is zero, the basic orbit is a bifurcation of the family and first order equations by themselves do not show how many (complex) branches come out of the ramification orbit, and more important, how many of them are *real* analytical continuations of the family.

Corrector. Generally, we will find a better approximation of a nearby periodic orbit by solving the system (34) for $\gamma=0$. By iteration of this procedure we will eventually reach a periodic orbit without ever leaving the manifold $C=C_0$. The iteration runs into difficulties when there is the possibility of more than one nearby periodic orbit lying on the manifold $C=C_0$; i.e. when the determinant (36) is zero or too close to zero.

Along the lines that we briefly described above, the computation of a periodic

orbit requires that we integrate together the orbital differential equations for a selected set of initial conditions and Hill's equation for the basic displacements n_1 and n_2, and also that we perform the quadrature for p_1 and p_2. All these integrations and quadratures are carried out stepwise by recurrent power series (Steffensen 1956, 1957a, 1957b, Deprit & Price 1965, Deprit & Zahar 1966). When the time reaches the estimate T given for the period, the corrector scheme is applied and better approximations of the initial conditions and the period are found. The procedure is iterated until the orbit is considered as being periodic within an assigned tolerance. Then the entire integration is started all over again, but this time we also integrate the non-homogeneous Hill's equation to obtain n_3 and by the ensuing quadrature, the tangential displacement p_3. The predictor scheme is applied and gives us a tangent to the manifold of periodic orbits and the tangent to the period curve

$$\frac{\partial x_0}{\partial C}, \frac{\partial y_0}{\partial C}, \frac{\partial \dot{x}_0}{\partial C}, \frac{\partial \dot{y}_0}{\partial C}; \frac{dT}{dC}.$$

Then we choose an increment γ, and applying the corrections (35), move onto the manifold $C = C_0 + 2\gamma$.

TABLE III

Intrinsic characteristics of the branch $\mathcal{L}_4{}^l$

No.	C	T	dT/dC	Tr	
1	3·0035	21·135145501	44·573	1·406010	S
2	3·005	21·394562458	265·400	0·837077	S
3	3·006	21·691167446	324·936	−0·047526	S
4	3·007	22·044255110	382·998	−1·098921	S
5	3·008	22·464343523	463·328	−2·087024	U
6	3·009	22·995474640	624·410	−2·429962	U
7	3·00996	24·020833373	—	1·602601	S
	—	—	—	—	
8	3·00996	24·124033931	−8756·264	2·409252	U
9	3·009	24·877969227	−352·275	10·371926	U
10	3·008	25·147798673	−212·811	13·921406	U
11	3·007	25·328228293	−154·360	16·414051	U
12	3·006	25·464510375	−120·787	18·338345	U
13	3·005	25·573488168	−98·496	19·901650	U
14	3·004	25·663532948	−82·374	21·218807	U
15	3·003	25·739487500	−70·037	22·362413	U
16	3·002	25·804440683	−60·215	23·382022	U
17	3	25·909208022	−45·428	25·181662	U
18	2·995	26·075093957	−23·559	29·124244	U
19	2·985	26·202638347	−5·476	37·182175	U
20	2·98	26·219949044	−1·782	41·522367	U
21	2·95	26·162330000	3·303	68·102952	U
22	2·9	26·001163632	2·921	102·529583	U
23	2·85	25·871655810	2·292	120·305911	U
24	2·8	25·768790381	1·849	123·641267	U
25	2·75	25·684643486	1·533	116·340641	U
26	2·7	25·614096638	1·299	102·153147	U
27	2·65	25·553849044	1·118	84·296094	U
28	2·6	25·501678463	0·974	65·337117	U
29	2·5	25·415750047	0·757	31·287272	U
30	2·4	25·348128704	0·602	9·216494	U
31	2·35	25·319610623	0·539	3·750322	U
32	2·305	25·296472125	0·489	2·013658	U
B_1	2·300583	25·294319726	—	2·000000	

4. *The branch of long period orbits* ($\mathscr{L}_4^l$). Starting from the orbits given by the analytical expansion around the point L_4, we have followed numerically the branch $\mathscr{L}_4^l$ up to the bifurcation orbit B_1 where it meets the short period family $\mathscr{L}_4^s$. We give in Table III the results concerning the period curve and the first order stability. For each orbit, we enter the value of the Jacobi constant C, the period T, the derivative dT/dC as given by (35) and the stability index Tr, defined by the relation

$$Tr = n_1(T) + n_2(T).$$

When this index is in absolute value less (greater) than 2, the characteristic exponent is purely imaginary (real), which is frequently referred to by saying that the orbit has linear stability (linear instability), in which case we enter an S (a U) in the sixth column. The case $Tr = 2$ corresponds to the annulment of the determinant (36). From Table III the period curve, T versus C, is drawn in Figs. 2 and 3. The

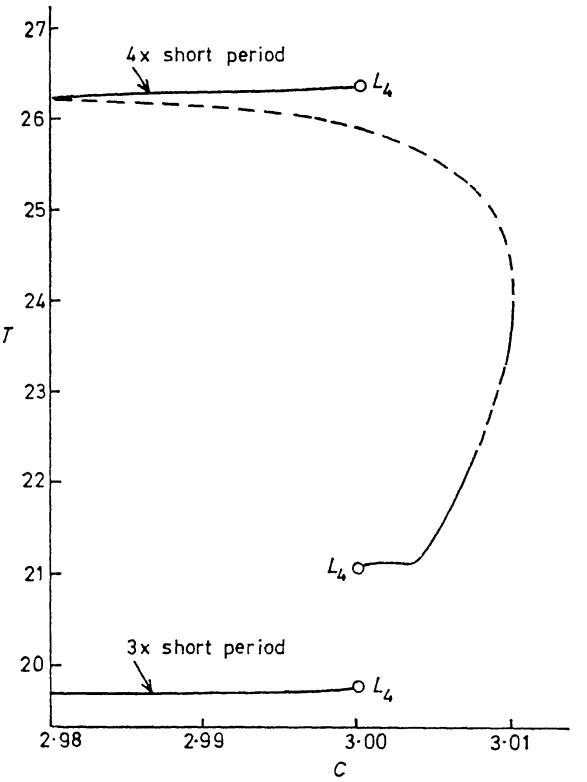

FIG. 2. *The period curve for* $\mathscr{L}_4^l$ *in the neighbourhood of the equilibrium.*

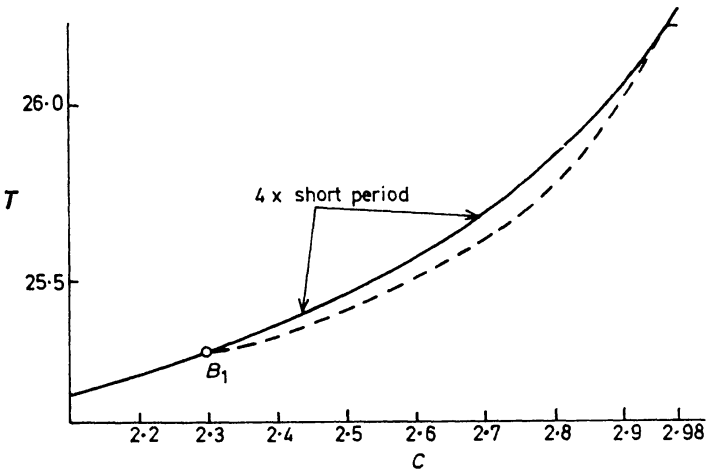

FIG. 3. *The period curve for* $\mathscr{L}_4^l$ *(continued).*

solid lines correspond to orbits with first order stability and the dashed lines to orbits with first order instability. In these figures we have also drawn the period curves of the short period orbits travelled three and four times (i.e. with the basic period multiplied by 3 and 4).

In Table IV, we enter a set of initial conditions (x_0, y_0, $\dot{x}_0$, $\dot{y}_0$) for each orbit. All these figures have been obtained in double precision arithmetic. Several functions which serve as a check in the course of the computation, like the Jacobi integral for the orbital equations and the Wronskian for Hill's equation, give evidence that the quantities entered in the tables can be found to at least 11 significant figures.

TABLE IV

Initial conditions for the branch $\mathscr{L}_4{}^l$

No.	x_0	y_0	$\dot{x}_0$	$\dot{y}_0$
1	0·494050076	0·977910758	0·149215754	−0·054919858
2	0·507396097	1·012800883	0·201524769	−0·083454244
3	0·512405341	1·024756987	0·217237020	−0·095921375
4	0·516360218	1·033606182	0·227836282	−0·106473701
5	0·519836776	1·040954368	0·235814421	−0·116433037
6	0·523163185	1·047597479	0·242133500	−0·126965897
7	0·528098017	1·056630699	0·249221205	−0·145591939
8	0·576620485	1·026776464	0·232584018	−0·160936225
9	0·581416004	1·033339813	0·238024091	−0·178807439
10	0·584891378	1·037839987	0·244030785	−0·188659522
11	0·588245748	1·042106229	0·250458033	−0·196976479
12	0·591544917	1·046255473	0·257104080	−0·204454802
13	0·594776822	1·050319927	0·263849839	−0·211344653
14	0·597953704	1·054286280	0·270599528	−0·217780353
15	0·601066536	1·058815424	0·277296887	−0·223841425
16	0·604108706	1·061923017	0·283903324	−0·229583137
17	0·609965983	1·069162922	0·296746251	−0·240266164
18	0·623265885	1·085595193	0·326219938	−0·263503507
19	0·644975332	1·112518834	0·374215068	−0·300992247
20	0·653999012	1·123737498	0·393858443	−0·317007259
21	0·694011593	1·173095324	0·477517243	−0·393441011
22	0·735500418	1·222745972	0·558728889	−0·483601882
23	0·763105804	1·254389866	0·610428854	−0·551426370
24	0·783188373	1·276460734	0·647373839	−0·606714169
25	0·798162512	1·292521080	0·675368101	−0·653646257
26	0·809429240	1·304216355	0·697086978	−0·694571133
27	0·817698589	1·312555495	0·714095400	−0·730849058
28	0·823378278	1·318135836	0·727307801	−0·763354355
29	0·827485503	1·322262941	0·744203619	−0·819073126
30	0·820762807	1·316328790	0·747429619	−0·863928747
31	0·810304875	1·307355436	0·740516843	−0·881462901
32	0·784650823	1·286181796	0·714541006	−0·889300818
B_1	0·770867229	1·275071808	0·697984995	−0·885130287

The family $\mathscr{L}_4{}^l$ has already been computed in the immediate neighbourhood of L_4 by Rabe & Schanzle (1962), who were the first to discover that the period curve goes through two relative extrema at about $C=3\cdot002$ (a maximum for T) and $C=3\cdot003$ (a minimum for T). As they took too large steps for their orbital parameter d_0, Rabe & Schanzle failed to detect the small portion of the family between $C=3\cdot008$ and $C=3\cdot0095$ along which the characteristic exponents change from stable to unstable type.

The last orbit these authors computed is at $C=3\cdot009753$ somewhat before the maximum value $3\cdot00996$ reached by C along $\mathscr{L}_4{}^l$. Beyond this maximum Wolaver (1963) has produced three more orbits, which he kindly communicated to us. His results have helped us to make certain that the branch goes through an extremum of C and to proceed beyond that point up to its natural termination.

Besides the two inner loops already discovered by Rabe & Schanzle the orbits start developing a third one while the Jacobi constant decreases monotonically, the period and the stability index both increase at first, go through a maximum, and then decrease monotonically. For the orbit B_1, for $C=2\cdot300583\ldots$, the stability index is equal to 2 and all solutions of Hill's equation are periodic, which

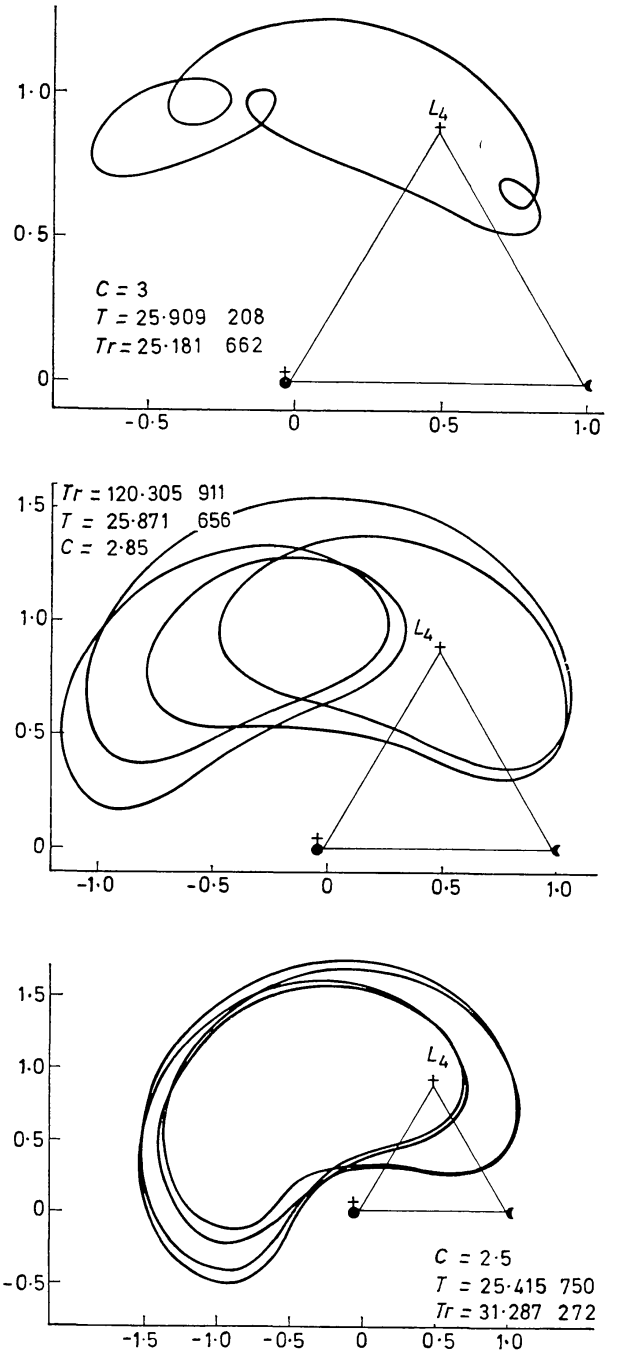

FIG. 4. *Evolution of the branch* $\mathscr{L}_4{}^l$.

indicates that we have reached here a bifurcation orbit in the manifold. The period $T=25\cdot294320$ is, as we shall see, exactly four times that of the short period orbit for that value of C. Morphologically speaking, what happens is that the three inner loops have inflated so much that, at the end, they come to coincide with each other and with the outer loop which is the backbone of the orbit. In conformity with Wintner's theorem (1931), we have checked that the characteristic exponent of the bifurcation orbit is indeed the argument of a fourth root of unity. In Fig. 4, we have attempted to put in evidence this morphological evolution by plotting in sequence three of the long period orbits between $C=3$ and $C=2\cdot5$.

5. *The branch $\mathscr{L}_4^s$ of short period orbits.* We have followed numerically the branch $\mathscr{L}_4^s$ up to the bifurcation orbit B_2 where it meets the branch $\mathscr{L}_5^s$—its symmetric with respect to the x axis—and the branch $\mathscr{L}_3$ emanating from L_3. Tables V and VI summarize the results we have obtained. The entries are the same as in Tables III and IV except for the derivative dT/dC which has not

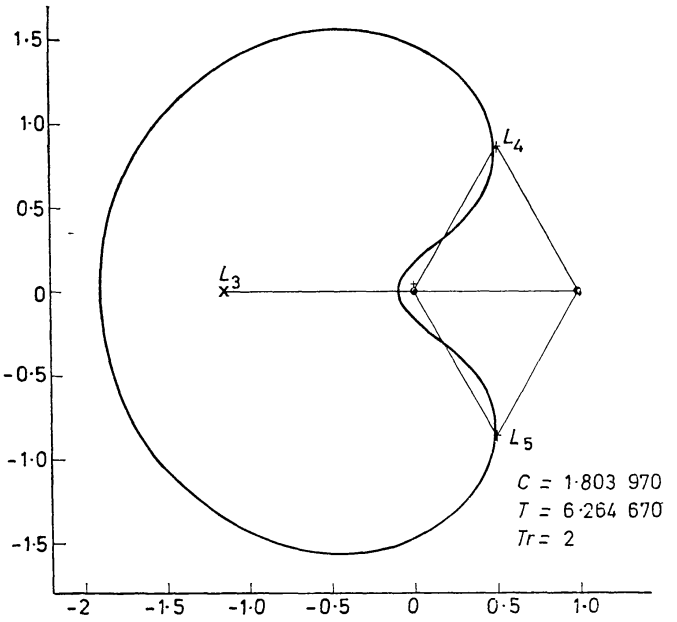

FIG. 5. *The bifurcation orbit B_2 at which $\mathscr{L}_4^s$ and $\mathscr{L}_5^s$ meet $\mathscr{L}_3$.*

been computed. Indeed those orbits have been established in the winter of 1965 by a program based on the numerical integration of the full resolvent in Cartesian coordinates (Deprit & Price 1965): in this case the period T rather than the Jacobi constant C was used as the parameter describing the family. We had not yet found how to obtain estimates of derivatives of initial conditions with respect to the period, so that we had no ' predictor ' equations. The equations used to improve an orbit (assuming a given period) were similar to the ' corrector equations ' described here. The branch $\mathscr{L}_4^s$ in the system Earth–Moon follows the same evolution as in the system Sun–Jupiter. We refer here the reader to the figures published by Goodrich (1966). However, this author had not reached the bifurcation orbit B_2 where the branches $\mathscr{L}_4^s$ and $\mathscr{L}_5^s$ meet $\mathscr{L}_3$. For this reason we thought it would be informative to reproduce B_2 (Fig. 5).

TABLE V

Intrinsic characters of the branch $\mathcal{L}_4^s$

No.	*C*	*T*	*Tr*	
1	2·97718203	6·56449572	−0·982689	*S*
2	2·92441143	6·52804058	−1·352199	*S*
3	2·86583772	6·49430522	−1·585730	*S*
4	2·81360276	6·46858364	−1·673695	*S*
5	2·75392624	6·44304123	−1·668058	*S*
6	2·68309964	6·41689621	−1·551168	*S*
7	2·65696886	6·40819809	−1·484728	*S*
8	2·57293886	6·38309377	−1·208781	*S*
9	2·53558834	6·37315622	−1·063021	*S*
10	2·48363824	6·36040664	−0·844042	*S*
11	2·42270712	6·34686290	−0·570766	*S*
12	2·34907456	6·33226400	−0·227985	*S*
B_1	2·30058300	6·32357993	0	*S*
13	2·09264163	6·29317422	0·938920	*S*
14	2·02	6·28471562	1·237378	*S*
15	1·92	6·27456468	1·614728	*S*
B_2	1·80397	6·26466965	2	*

TABLE VI

Initial conditions for the branch $\mathcal{L}_4^s$

No.	x_0	y_0	$\dot{x}_0$	$\dot{y}_0$
1	0·54470261	1·02516301	0·26826223	−0·16053814
2	0·51191132	1·18530021	0·48774813	−0·24532608
3	0·54948245	1·25590466	0·60011038	−0·34583506
4	0·57407370	1·29777781	0·66691701	−0·41550094
5	0·59579127	1·33207680	0·72266665	−0·48168296
6	0·61522429	1·36084892	0·77125197	−0·54786532
7	0·62106494	1·36903198	0·78568950	−0·56978667
8	0·63566755	1·38876297	0·8228611	−0·63317781
9	0·64035583	1·39485579	0·83569444	−0·65847659
10	0·64267540	1·40311940	0·85317742	−0·68920838
11	0·64868531	1·40529295	0·86372206	−0·72662252
12	0·64972270	1·40652607	0·87464135	−0·76561064
B_1	0·77086737	1·27507192	0·69798518	−0·88513033
13	0·62486907	1·37813303	0·87031469	−0·87748962
14	−1·46244012	1·15213671	1·00177663	1·23702472
15	−1·47478141	1·16217845	1·06796705	1·24241179
B_2	−1·91179867	0	0	1·70628875

In the system Earth–Moon, as we have said before, contrary to Brown's conjecture for infinitesimally small mass ratios, the branch $\mathcal{L}_4^l$ terminates at B_1 which is an element of $\mathcal{L}_4^s$. This remarkable short period orbit is reproduced in Fig. 6.

Along the branch $\mathcal{L}_4^s$, both the Jacobi constant and the period decrease monotonically, while the stability index, *Tr*, first decreases, goes through a minimum and then increases monotonically without ever leaving the interval $(-2, +2)$ corresponding to the so-called linear stability. The period curve, *T* versus *C*, is shown in Fig. 9 together with the period curve of the branch $\mathcal{L}_3$.

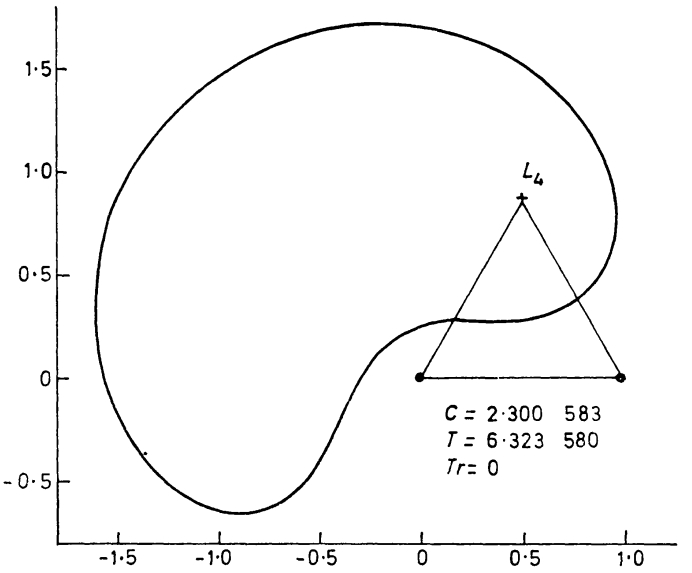

FIG. 6. *The bifurcation orbit B_1 at which $\mathcal{L}_4^s$ and $\mathcal{L}_4^l$ meet.*

6. *Numerical continuation in parabolic coordinates.* In order to investigate the branch $\mathcal{L}_3$ which contains an ejection orbit from the Earth we use a predictor–corrector scheme similar to the previous one but based upon the description of the Restricted Problem by a regularizing set of coordinates and time, namely the parabolic regularization. The new coordinates ξ, η and time s are related to the Cartesian ones by the identities

$$x=\xi^2-\eta^2, \qquad y=2\xi\eta, \qquad dt=4(\xi^2+\eta^2)ds. \tag{38}$$

Through this transformation the Cartesian equations (19) are transformed into the differential equations

$$\xi''-8\rho\eta'=\frac{\partial W}{\partial \xi}$$

$$\eta''+8\rho\xi'=\frac{\partial W}{\partial \eta} \tag{39}$$

where

$$W=2\rho^3+2(\mu-C)\rho-4\mu(\xi^2-\eta^2)\rho+4\mu\frac{\rho}{\sigma}+4(1-\mu),$$

$$\rho=\xi^2+\eta^2, \qquad \sigma^2=\rho^2-2(\xi^2-\eta^2)+1. \tag{40}$$

According to Painlevé's theorem of duality, any solution of (39) which lies on the manifold

$$K=2W-\xi'^2-\eta'^2=0 \tag{41}$$

corresponds to a solution of (19) belonging to the energy manifold defined by giving the value C to the Jacobi constant in (21). (Note that W and consequently the right-hand members of (39) depend explicitly on C.) Conversely any solution of (19) on this energy manifold corresponds to a solution of (39) which lies on the manifold (41). We have shown in another paper (Deprit & Henrard 1967) how this duality is to be extended to the displacements of the orbits through that iso-

energetic reduction on which the regularization for fixed binary collisions is based. Let us assume that

$$\xi(s),\ \eta(s) \tag{42}$$

is a solution of (39) with $C=C_0$ and belongs to the manifold (41). The displaced trajectories we shall consider are solutions of equation (39) with $C=C_0+2\gamma$ and belong to the manifold (41). As we did before we describe them by their normal and tangential displacements with respect to (42) and we make the assumption that the products of those quantities and of γ are negligible. Hence the normal displacement is a solution of the non-homogeneous form of Hill's equation

$$n''+\theta n=\Psi.\gamma, \tag{43}$$

where, in parabolic coordinates, θ and Ψ are functions of the time s defined by the relations,

$$\theta=V''/V+2(4\rho+\phi')^2-8\left[5\rho^2+6(\eta^2-\xi^2)+2(\xi\eta'-\eta\xi')+\frac{2\mu}{\sigma^3}+\mu-C\right],$$

$$\Psi=8[(\xi\eta'-\eta\xi')+\rho(4\rho+\phi')]/V.$$

To each normal displacement $n(s)$ corresponds a tangential displacement $p(s)$ with $p(0)=0$ given by the quadrature

$$p(s)=V(s)\int_0^s 2[n(w).(4\rho(w)+\phi'(w))/V(w)-2.\gamma.\rho(w)/V^2(w)]dw.$$

The general solution of Hill's equation can be integrated by recurrent power series together with the orbital equations (39) as for the Cartesian coordinates, and leads to the same system of equations for the predictor and the corrector. But the orbits we have to deal with here are symmetrical with respect to the η-axis: we have shown elsewhere (Deprit & Henrard 1967) how to set up the equations for prediction and correction so that the orbit and its displacements be computed for only half the period and it is precisely these time-saving predictors and correctors that we have been using here. In particular, the predictor yields the following functions,

$$\frac{\partial\xi_0}{\partial C}=0,\quad \frac{\partial\eta_0}{\partial C},\quad \frac{\partial\xi_0'}{\partial C},\quad \frac{\partial\eta_0'}{\partial C}=0,\quad \frac{dS}{dC};$$

S indicating here the period as referred to the regularizing time variable s.

7. *The branch $\mathscr{L}_3$ of librations emanating from L_3.* In order to study the periodic orbits in the vicinity of the equilibrium L_3, we translate the origin of the synodical coordinates and their conjugate momenta to the equilibrium point itself:

$$\begin{aligned} x&=x_L+X & p_x&=P_X\\ y&=Y & p_y&=x_L+P_Y. \end{aligned} \tag{44}$$

Note that x_L represents the barycentric synodical abscissa of L_3. The Hamiltonian function (1) becomes

$$H=\tfrac{1}{2}(P_X{}^2+P_Y{}^2)-(XP_Y-YP_X)-\Omega \tag{45}$$

where the force function $\Omega(X, Y)$ is defined by

$$\Omega(X, Y)=x_L.X+\frac{1-\mu}{\rho_1}+\frac{\mu}{\rho_2}. \tag{46}$$

According to Liapunov's theorem, one and only one family of periodic orbits emanates from L_3. In the neighbourhood of L_3, this family can be expanded in power series of an orbital parameter ϵ:

$$\begin{aligned} X(\tau, \epsilon) &= \sum_{m \geqslant 1} X_m(\tau)\epsilon^m, \\ Y(\tau, \epsilon) &= \sum_{m \geqslant 1} Y_m(\tau)\epsilon^m. \end{aligned} \tag{47}$$

The functions $X_m(\tau)$ and $Y_m(\tau)$ are Fourier sums in τ which is a new time variable defined by the relation:

$$\tau = \omega t = \frac{\omega_0}{1+\nu} t \tag{48}$$

where $i\omega_0$ is the imaginary characteristic exponent at the equilibrium, and ν is a power series in the orbital parameter:

$$\nu = \sum_{m \geqslant 1} \nu_m \epsilon^m. \tag{49}$$

The coefficients in the power series (47) and (49) have the same parity properties (6) as the coefficients of the expansion (3) and (5) around L_4. Hence it is not difficult to show that:

(a) The family issuing from L_3 is a natural family of periodic orbits, except at the equilibrium L_3 which is a singularity;

(b) The orbital parameter ϵ is an analytical coordinate which renders uniform the local equilibrium;

(c) The family admits a unique real continuation through the equilibrium ($\epsilon = 0$) but it is a reflexion of the branch upon itself.

As the equilibrium is located on the x-axis, the force function (46) shows a symmetry

$$\Omega(X, Y) = \Omega(X, -Y).$$

This character is instrumental in proving that the expansion (47) has the symmetry properties

$$\begin{aligned} X(\tau, \epsilon) &= X(-\tau, \epsilon) \\ Y(\tau, \epsilon) &= -Y(-\tau, \epsilon), \end{aligned} \tag{50}$$

provided that the initial time has been chosen in a consistent way. This choice of the initial time is actually performed when we build the critical terms at each odd order of the expansion which is carried out in the same way as it was done for the expansion around L_4. With the same notation as in the second paragraph, we have to take as particular solution for the critical terms

$$\tilde{X}_{2M+1}(\tau) = A \cos \tau, \qquad \tilde{Y}_{2M+1}(\tau) = B \sin \tau.$$

The symmetry is also responsible for the disappearance of the test on the absolute accuracy of the coefficients of the mean motion ω. Indeed each of those coefficients is the solution of only one linear equation. We shall use instead a control on the absolute accuracy of the computation of the Jacobi constant. Indeed each order of the Jacobi constant comes out of the computation as a Fourier sum of which all the coefficients except the independent one should be zero. At each even order we shall take the largest of them as a control of accuracy and enter it in the third

column of Table VII after the coefficients of the Jacobi constant and of the mean motion.

TABLE VII

Series for the periodic librations at L_3

	Jacobi constant C	Mean motion ω	Test on C
ϵ^0	3·02412841	1·01041066	—
ϵ^2	−1·06366970	−0·00603950	4×10^{-15}
ϵ^4	0·56345559	0·00336505	7×10^{-14}
ϵ^6	−0·92444139	−0·00574305	1×10^{-13}
ϵ^8	1·62493472	0·00993688	2×10^{-13}
ϵ^{10}	−3·24898220	−0·01995166	7×10^{-13}
ϵ^{12}	6·91142699	0·04242085	3×10^{-12}
ϵ^{14}	$-1\cdot53896793\times10$	−0·09449198	7×10^{-11}
ϵ^{16}	$3\cdot53992396\times10$	0·21737976	2×10^{-10}
ϵ^{18}	$-8\cdot34659865\times10$	−0·51261779	6×10^{-9}
ϵ^{20}	$2\cdot00655483\times10^2$	1·23248394	1×10^{-8}
ϵ^{22}	$-4\cdot89984919\times10^2$	−3·00988882	2×10^{-7}
ϵ^{24}	$1\cdot21199751\times10^3$	7·44563606	4×10^{-6}
ϵ^{26}	$-3\cdot03039570\times10^3$	$-1\cdot86175026\times10$	1×10^{-5}

The series truncated at order 27 yield a good approximation of the branch $\mathscr{L}_3$ over a large neighbourhood of the equilibrium as it may be seen in Table VIII where, for several values of ϵ, we enter the Jacobi constant, the corrections to be added to the period and the initial abscissa in order to obtain the true periodic orbit and in the last column the difference between the maximum and the minimum values of y, which is an estimate of the diameter of the orbit.

TABLE VIII

Test on the approximation of $\mathscr{L}_3$ by series (Truncated at order 27)

ϵ	C	ΔT	Δx_0	$y_M - y_m$
0·15	3·000471	—	—	0·6
0·35	2·900880	3×10^{-12}	2×10^{-9}	1·3
0·48	2·800813	2×10^{-8}	1×10^{-5}	1·7
0·59	2·695817	4×10^{-6}	2×10^{-3}	2·0
0·66	2·590838	8×10^{-5}	4×10^{-2}	2·2

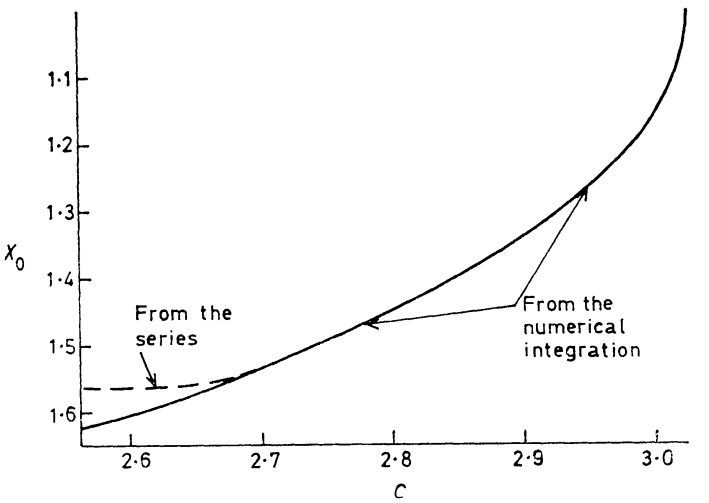

FIG. 7. *The curve of initial abscissas for $\mathscr{L}_3$.*

In Fig. 7 is plotted the initial abscissa versus the Jacobi constant. The dashed curve is computed from the series and the solid one from numerical integration. One can observe that, after a long interval on which they agree closely the two curves suddenly depart sharply from each other. This could be explained by the fact that the series in C and x_0 are alternating. However, the break occurs relatively far from the equilibrium and the truncated series cover orbits which can no longer be looked at as infinitesimally small librations. As an instance, we produce in Fig. 8 an orbit of the branch $\mathscr{L}_3$ which we consider as the farthest one in the family to be described adequately by the series.

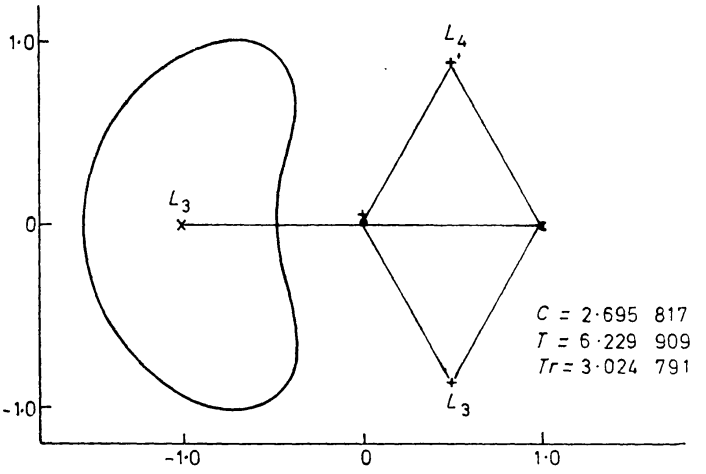

FIG. 8. *The largest periodic libration around L_3 produced from the series.*

We have followed the branch $\mathscr{L}_3$ all the way to the first ejection orbit E_1 from the Earth and even beyond it. The significant results are entered in Tables IX and X. Table IX contains the intrinsic characteristics of the orbits: the Jacobi constant C, the period T in the time t, the period S in the regularized time s, the derivative dS/dC and the stability index Tr, a quantity which is invariant with respect to not only an analytical coordinate transformation but also a transformation of the time as defined here (Poincaré 1892).

TABLE IX

Intrinsic characteristics of the branch $\mathscr{L}_3$

No.	C	T	S	dS/dC	Tr	
1	3·024	6·218398467	1·565696973	−0·0109	3·353170	U
2	3·02	6·218538337	1·565740437	−0·0109	3·349088	U
3	3·01	6·218887918	1·565848750	−0·0108	3·338896	U
4	3	6·219237373	1·565956565	−0·0108	3·328724	U
5	2·7	6·229717706	1·568971788	−0·0094	3·029830	U
6	2·5	6·236816193	1·570766430	−0·0086	2·831058	U
B_2	1·803970	6·264669649	1·575969990	−0·0066	2	—
7	1·4	6·28564481 1	1·578458932	−0·0058	1·211073	S
E_1	1·042903	6·308355261	1·580491447	−0·0057	0·059769	S
8	0·897954	6·318368208	1·581337849	−0·0060	−0·611567	S

In Table X we have entered the value of the coordinate η and the velocity ξ' at a time when the orbit crosses the η axis at the one of the two points which is

farther away from the Earth. Hence, as the orbits are symmetrical, ξ and η' should be taken as being zero to complete the set of initial conditions.

TABLE X

Initial conditions for the branch $\mathscr{L}_3$

No.	η	ξ'
1	1·002370279	0·047810494
2	1·027287924	0·255390805
3	1·052620164	0·477265305
4	1·069155284	0·628199075
5	1·234432344	2·440789461
6	1·284983478	3·131122388
B_2	1·378277420	4·703478500
7	1·401973067	5·273046969
E_1	1·409961794	5·619802665
8	1·409859816	5·720321995

The period curve, T versus C, is drawn in Fig. 9, together with the period curve of the branch $\mathscr{L}_4{}^s$ of asymmetric orbits. As a matter of fact, the latter is also the period curve of the branch $\mathscr{L}_5{}^s$. Indeed orbits being symmetrical with respect to each other have the same intrinsic characters.

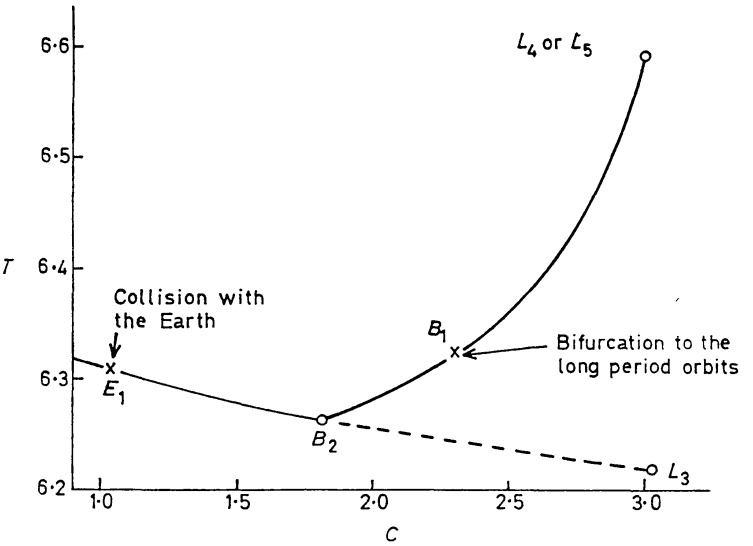

FIG. 9. *The period curve for $\mathscr{L}_4{}^s$, $\mathscr{L}_5{}^s$ and $\mathscr{L}_3$.*

Along the branch $\mathscr{L}_3$, from L_3 down to beyond the ejection orbit E_1, the Jacobi constant decreases monotonically while the period increases. The trace decreases and passes from the unstable type to the stable type through the bifurcation orbit B_2, which is of the type that Wintner calls indifferent stability. After B_2, it goes on decreasing, but remains of the stable type through the ejection orbit E_1. This ejection orbit E_1 is remarkable. To our knowledge, it is the first instance of a periodic collision orbit whose characteristic exponents are undoubtedly of the stable type. For this reason, we present it in Fig. 10.

The branch $\mathscr{L}_3$ has been followed all the way by Broucke (1963). He states that the family meets that of the retrograde orbits of the first kind around the Earth which he calls A_1 on a bifurcation orbit. Since then, from computing the

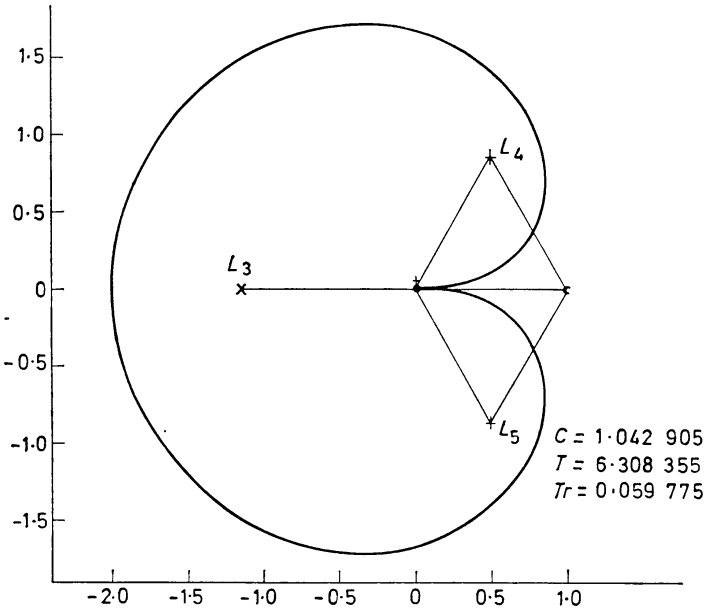

FIG. 10. *The ejection orbit E_1 from the Earth.*

characteristic exponents, Broucke has shown that the branching orbit is indeed of odd indifferent stability ($Tr(T) = -2$) when it is considered within the family A_1, whereas, in the family $\mathscr{L}_3$, it appears as an orbit travelled twice, having thus, in agreement with Wintner's theorem, the even indifferent stability ($Tr(2T) = 2$).

8. *Conclusions.* The Trojan manifold of periodic orbits in the system Earth–Moon comprises among its branches the natural families $\mathscr{L}_4{}^s$, $\mathscr{L}_4{}^l$, $\mathscr{L}_5{}^s$, $\mathscr{L}_5{}^l$ and $\mathscr{L}_3$. It has at least three natural terminations, namely the equilibrium configurations L_4, L_5 and L_3, and at least three bifurcations, namely the orbit B_1 where $\mathscr{L}_4{}^s$ and

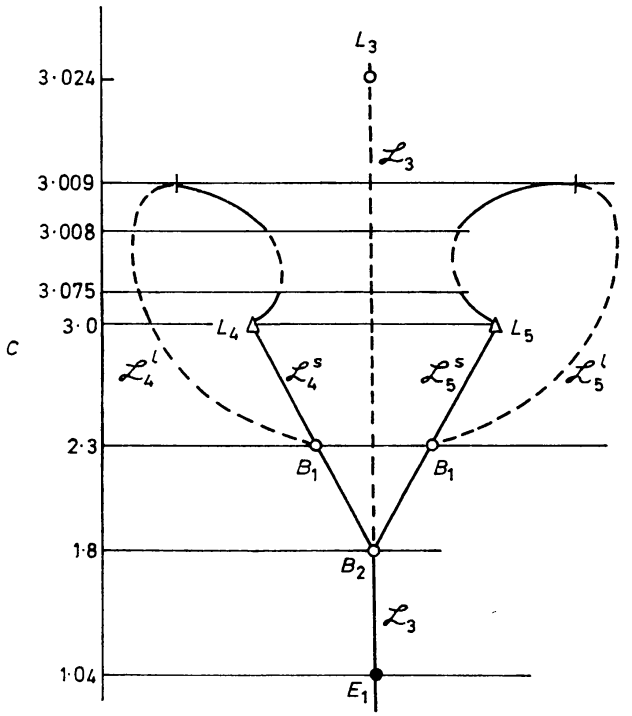

FIG. 11. *Genealogy tree of the Trojan manifold.*

$\mathscr{L}_4{}^l$ meet, the symmetrical orbit B_2 where $\mathscr{L}_4{}^s$, $\mathscr{L}_5{}^s$ and $\mathscr{L}_3$ branch out, and the image of B_1 by the involution $(x, y, t) \rightarrow (x, -y, -t)$ where $\mathscr{L}_5{}^s$ and $\mathscr{L}_5{}^l$ meet.

The numerical findings are best visualized in the genealogical tree drawn in Fig. 11. The various values of the Jacobi constant C are ordered along the vertical axis in decreasing order without paying attention to the scale; no physical quantity is attached to the horizontal axis. A point in this diagram represents a periodic orbit. Two periodic orbits having the same Jacobi constant are situated on the same vertical level. To signify that two periodic orbits belong to the same natural family, we link their representative points by a curve made of the points which stand for the periodic orbits in the connecting family. Families are represented by solid lines as long as the characteristic exponents of their constituent orbits are of the stable type, and by dashed lines when the characteristic exponents are of the unstable type. Bifurcation orbits are indicated by hollow circles, and ejection orbits by full disks.

Concerning the genealogy of the branches so far explored in the Trojan manifold of periodic orbits in the system Earth–Moon, we have to add two comments.

(a) We have not inquired about the order of the ramification either at the bifurcation orbit B_1 or at B_2. At least we can say that, as far as B_2 is concerned, the situation conforms to the conclusions drawn by Poincaré (1899) out of his analysis of the branchings for a natural manifold of periodic orbits. But this does not preclude the existence of more pairs of real branches coming out of B_2 in the direction of either increasing or decreasing Jacobi constants. In the case of B_1, we know from Poincaré's discussion that, besides the families of long and short period orbits, there should be a third branch with stable characteristic exponents in the direction of increasing Jacobi constants. Once an orbit has been found on that branch, we do not expect it too difficult to continue this missing family by predictor and correctors. But it may prove to be an arduous task to extricate the first orbit.

(b) All periodic collision orbits computed by Hénon (1965) in the Copenhagen problem ($\mu = \frac{1}{2}$) have characteristic exponents of the unstable type. It does not necessarily follow that such is the case for any periodic ejection orbit. In fact, we produce here, for the first time to our knowledge, a collision orbit with stable characteristic exponents.

Acknowledgments. The analytic continuation in d'Alembert series for the branches $\mathscr{L}_4{}^s$ and $\mathscr{L}_4{}^l$ around L_4 and for the branch $\mathscr{L}_3$ in the neighbourhood of L_3 was implemented on the IBM 7094 by A. R. M. Rom (Boeing Scientific Research Laboratories). Mrs André Deprit-Bartholomé assisted in programming the numerical continuation of the various branches of periodic orbits.

We thank Dr Roger Broucke (Jet Propulsion Laboratory), Dr J. M. A. Danby (Yale University Observatory) and Dr Eugene Rabe (University of Cincinnati Observatory) for discussions.

Dr Julian Palmore is indebted to the Boeing Company for support during the summer 1966 in its Scientific Research Laboratories.

Boeing Scientific Research Laboratories,
Seattle,
Washington.
1967 *April.*

References

Breakwell, J. & Pringle, R. J., 1966. Methods in Astrodynamics and Celestial Mechanics, *Progress in Astronautics and Aeronautics*, ed. by R. L. Duncombe and V. G. Szebehely, pp. 55–74, Academic Press, New York.

Broucke, R., 1963. *Dissertation présentée pour obtenir le grade de docteur en sciences*, University of Louvain, Belgium.

Brown, E. W., 1911. *Mon. Not. R. astr. Soc.*, **71,** 438–454.

Brown, E. W. & Shook, A. C., 1933. *Planetary Theory*, Cambridge University Press.

Burrau, C. L., 1894. *Astr. Nachr.*, **136,** 161–74.

Danby, J. M. A., Deprit, A. & Rom, A. R. M., 1965. Boeing Scientific Research Document D1–82–0481, Seattle, Washington.

Deprit, A. & Delie, A., 1965. *Icarus*, **4,** 242–66.

Deprit, A. & Price, J. F., 1965. *Astr. J., N.Y.*, **70,** 83–4.

Deprit, A. & Zahar, R. V. M., 1966. *Zeitsch. Ang. Math. Phys.*, **17,** 425–30.

Deprit, A., Henrard, J. & Rom, A. R. M., 1967. *Proceedings of the Space Flight Mechanics Conference* (*Denver, Colorado*) *AAS Science and Technology Series*, Vol. 12, Western Periodicals, North Hollywood, California, 85–105.

Deprit, A. & Henrard, J., 1967. *Astr. J., N.Y.*, **72,** 158–172.

Goodrich, E., 1966. *Astr. J., N.Y.* **71,** 88–93.

Hénon, M., 1965. *Ann. d'Astrophys.*, **28,** 992–1007.

Nemyskii, V. V. & Stepanov, V. V., 1960. *Qualitative Theory of Differential Equations*, Princeton University Press.

Pedersen, P., 1935. *Mon. Not. R. astr. Soc.*, **95,** 482–95.

Poincaré, H., 1892 and 1899. *Les Méthodes Nouvelles de la Mécanique céleste*, Vols. I and III, Gauthier-Villars, Paris.

Rabe, E. & Schanzle, A., 1962. *Astr. J., N.Y.*, **67,** 732–9.

Schutz, B. E., 1966. Thesis for the Degree of Master of Science, Graduate School of the University of Texas.

Steffensen, J. F., 1956a. *Acta Math.*, **95,** 25–37.

Steffensen, J. F., 1956b. *Det Kong. Danske Vidensk. Selskab, Mat. Fys. Medd.*, **30,** No. 18.

Steffensen, J. F., 1957. *Det Kong. Danske Vidensk. Selskab, Mat. Fys. Medd.*, **31,** No. 3.

Steg, L. & de Vries, J. P., 1966. *Space Sc. Rev.*, **5,** 210–33.

Stumpff, K., 1965. *Himmelsmechanik*, Veb Deutscher Verlag der Wissenschaften, Berlin.

Wintner, A., 1931. *Am. J. Math.*, **53,** 605–25.

Wintner, A., 1941. *Analytical Foundations of Celestial Mechanics*, Princeton University Press.

Wolaver, L., 1963. Private communication in the form of a letter to Professor Rabe.